Evaluation of ^{18}F-FDG PET with Bladder Irrigation in Patients with Uterine and Ovarian Tumors

Koichi Koyama, MD[1]; Terue Okamura, MD[1]; Joji Kawabe, MD[2]; Nozomi Ozawa, MD[1]; Kenzi Torii, MD[1]; Naohiko Umesaki, MD[3]; Masato Miyama, MD[3]; Hironobu Ochi, MD[2]; and Ryusaku Yamada, MD[1]

[1]Department of Radiology, Osaka City University School of Medicine, Osaka, Japan; [2]Department of Nuclear Medicine, Osaka City University School of Medicine, Osaka, Japan; and [3]Department of Obstetrics and Gynecology, Osaka City University School of Medicine, Osaka, Japan

The purpose of this study was to evaluate PET using ^{18}F-FDG for gynecologic lesions with continuous bladder irrigation to eliminate artifacts from the ^{18}F-FDG activity in the bladder. **Methods:** Forty-one patients were studied. They had 23 cervical uterine lesions (15 cases of cancer, 5 recurrences, 3 nonrecurrences); 8 cases of uterine corpus cancer, including 2 recurrences; and 10 ovarian masses (6 malignant, 4 nonmalignant). All cases of cancer were histologically proven; however, 2 cases of nonrecurrent uterine cervical carcinomas were diagnosed by clinical course. Continuous bladder irrigation was performed 35–55 min after intravenous administration of 185–370 MBq ^{18}F-FDG, and an emission scan was obtained 40–55 min after intravenous administration. Standardized uptake value (SUV) was used to estimate the degree of ^{18}F-FDG uptake quantitatively. **Results:** After bladder irrigation, the ^{18}F-FDG activity in the urinary tract was eliminated in 33 patients, so that detection of tumor ^{18}F-FDG accumulation was easy. Two patients showed residual activity in the urinary bladder, and 6 patients showed activity in the ureter. An artifact was seen in 1 patient with residual activity in the urinary bladder caused by insufficient irrigation. However, these residual activities had no influence on detecting ^{18}F-FDG accumulation in tumor. The mean (±SD) of SUVs of malignant lesions was 6.04 ± 3.22, that of nonmalignant lesions was 1.71 ± 1.12, and the difference was significant ($P = 0.0002$). SUVs of all malignant lesions were greater than 2.0, and SUVs of all nonmalignant lesions, except the 1 case of ovarian fibroma, were less than 2.0. **Conclusion:** ^{18}F-FDG PET with continuous bladder irrigation is useful for eliminating ^{18}F-FDG activity in the bladder and for differentiating between malignant and nonmalignant uterine or ovarian masses.

Key Words: ^{18}F-FDG PET; bladder irrigation; uterine cancer; ovarian tumor; MRI

J Nucl Med 2003; 44:353–358

Received Apr. 11, 2002; revision accepted Oct. 4, 2002.

For correspondence or reprints contact: Koichi Koyama, MD, Department of Radiology, Osaka City University, 1-5-7, Asahi-Machi, Abeno-ku, Osaka, 545-8585, Japan.

E-mail: koichikoyamats@yahoo.co.jp

For the diagnosis of malignant tumors, PET using ^{18}F-FDG is a useful nuclear medicine imaging tool. FDG is a glucose analog marked by ^{18}F while being taken up by viable cells and is phosphorylated by intracellular hexokinase (*1*). FDG-6 phosphate undergoes no further metabolism and is accumulated in cells as FDG-6 phosphate. Glucose metabolism and hexokinase activity are known to be increased in malignant cells (*2*). ^{18}F-FDG thus accumulates in malignant tumors, and ^{18}F-FDG PET can assess glucose metabolic activity in tumors noninvasively (*1–4*). The usefulness of ^{18}F-FDG PET has been reported for the diagnosis of various kinds of tumors (*5*), and standardized uptake value (SUV) was used for the quantitative analysis of ^{18}F-FDG PET.

The high ^{18}F-FDG activity in urine creates an annoying artifact in the diagnosis of pelvic lesions. High ^{18}F-FDG activity in the urinary bladder is especially a problem, because gynecologic tumors usually exist adjacent to the urinary bladder. ^{18}F-FDG PET is therefore seldom performed for gynecologic tumors, and there have been only a few reports on such use of ^{18}F-FDG PET (*6–12*).

The purpose of this study was to evaluate the usefulness of ^{18}F-FDG PET with continuous urinary bladder irrigation to eliminate the artifact from the urinary bladder in patients with gynecologic lesions. The optimal SUV cutoff to clinically distinguish malignant from nonmalignant lesions was also investigated.

MATERIALS AND METHODS

From August 1997 to March 2000, we studied 41 women (age range, 26–84 y; mean age, 55.6 y) who were suspected to have gynecologic tumors because of clinical findings or the findings of several imaging modalities. All patients underwent MRI of the pelvis with a 1.5-T MRI system and ^{18}F-FDG PET before treatment.

Of the 34 cases of malignancy, 12 were recurrent. The 22 nonrecurrent malignancies comprised 15 cases of uterine cervical carcinoma, 6 of uterine corpus carcinoma, and 1 of ovarian serous cystadenocarcinoma. The 12 recurrent malignancies comprised 5

cases of uterine cervical carcinoma, 2 of uterine corpus carcinoma, and 5 of ovarian cancer. Seven patients had benign disease, consisting of 2 benign ovarian tumors (1 fibroma and 1 dermoid cyst), 2 cases of postoperative endometrial adenocarcinoma of the ovary, and 3 cases of nonrecurrent uterine cervical carcinoma (all were postoperative uterine cervical carcinoma with no recurrent tumors in the pelvic region). In all cases of recurrent or nonrecurrent carcinoma, at least 6 mo had passed after surgery and chemotherapy or radiotherapy. Thirty-nine cases were proven histologically, but 2 cases of nonrecurrent uterine cervical carcinoma were diagnosed through the clinical course.

^{18}F-FDG was produced with a superconducting cyclotron (NKK-Oxford, Tokyo, Japan) and synthesis system (NKK, Tokyo, Japan). A Headtome IV, model SET-1400W-10 (Shimadzu Corp., Kyoto, Japan), which has 4 detector rings providing 7 contiguous slices at 13-mm intervals, was used for the PET studies. The effective spatial resolution was 14 mm in full width at half maximum.

^{18}F-FDG PET was performed as follows. A Foley balloon catheter (14 or 16 French) (Hitachi Medical Corp., Tokyo, Japan) connected to a urine collection bag (JMS Corp., Tokyo, Japan) was first placed in the urinary bladder before the transmission scan. After performing the transmission scan for 10 min with a ^{68}Ge/^{68}Ga ring source for attenuation correction, we intravenously injected 185–370 MBq ^{18}F-FDG into the patients, who had been fasting for at least 4 h. Emission scanning was performed with continuous urinary bladder irrigation at between 40 and 55 min after intravenous injection. Continuous urinary bladder irrigation was performed manually using prewarmed physiologic saline solution contained in disposable syringes, beginning 5 min before the start of the emission scan and continuing until the end of the scan. Each disposable syringe contained 50 mL of physiologic saline solution and was used only once; the total amount of saline used was up to about 2 L. The patients were not given any diuretics. The ^{18}F-FDG PET images were reconstructed using filtered backprojection.

We investigated the ^{18}F-FDG PET images quantitatively. For the quantitative analysis, regions of interest (circles 6 mm in diameter) were placed in the areas of highest ^{18}F-FDG accumulation among suspected mass lesions, as determined by referring to the MR images, and mean SUVs were determined as follows: SUV = tissue concentration (MBq/g)/injected activity (MBq) per body weight (g).

SUVs were not corrected for partial-volume effects. The nonparametric Mann–Whitney U test was used to analyze data. A 2-tailed P value of less than 0.05 was considered significant.

RESULTS

No patients complained of pain during the urinary bladder irrigation. In 33 cases, the ^{18}F-FDG activity in the urinary tract was eliminated (Table 1) and the ^{18}F-FDG accumulation in the tumor was clearly seen. A typical case of uterine cervical carcinoma (patient 15) is shown in Figure 1. No patients had hydroureter or hydronephrosis, but residual radionuclide activity in the urinary system was noted in 8 patients, 2 of whom showed activity in the urinary bladder and 6 in the ureter (Table 1). In only 1 patient (patient 33), there was an intense artifact in the urinary bladder because of residual activity (Fig. 2A). In this patient, we failed to sufficiently irrigate the bladder because the balloon catheter did not work well. In the other patient with activity in the urinary bladder, the activity was low, but the reason for its presence was not clear. In these 2 patients, the slice level of the ^{18}F-FDG accumulation in the tumor was not the same as the slice level of the residual activity in the urinary bladder; these residual activities therefore had no effect on detecting ^{18}F-FDG accumulation in the tumor. In the 6 patients with residual activity in the ureter, it was sometimes difficult to differentiate the residual activity from ^{18}F-FDG uptake by lymph node metastases or the primary lesion. In 1 patient with residual activity in the ureter, shown in Figure 2B (patient 24), the residual activity was also difficult to differentiate using axial images alone but was easy to differentiate by referring to MR images or by reconstructing coronal ^{18}F-FDG PET images (Fig. 2C).

The SUVs for all patients were between 0.26 and 13.58 (Table 1), and the distribution of SUVs is shown in Figure 3. The SUVs for patients with malignancy were between 2.09 and 13.48, with a mean ($\pm$SD) of 6.04 $\pm$ 3.22, and the SUVs for patients with nonmalignant disease were between 0.26 and 2.93, with a mean of 1.71 $\pm$ 1.12. There was a significant difference between malignant and nonmalignant cases (P = 0.0002). For differentiating between malignant and nonmalignant lesions, the SUV cutoff at which the highest accuracy was obtained was 2.0. When this cutoff value was used, sensitivity, specificity, positive predictive value, negative predictive value, and accuracy were 100%, 86%, 97%, 100%, and 98%, respectively. There was only 1 case of false-positivity at the 2.0 cutoff value; this case (of ovarian fibroma, in patient 39) is shown in Figure 4. One case of nonrecurrent uterine cervical carcinoma (patient 21) showed a low SUV of 0.26 because of the presence of a cystic mass lesion with a thin wall.

The distribution of SUVs for each gynecologic mass is shown in Figure 5. No significant difference was found between the SUVs for uterine cervical cancer and those for uterine corpus cancer. The SUVs for recurrent uterine cervical carcinoma showed a tendency to be low, whereas the SUVs for recurrent uterine corpus carcinoma showed a tendency to be high. However, there were only 2 cases of recurrent uterine corpus carcinoma. The presence of a significant difference in SUVs between cases of primary ovarian cancer and cases of benign ovarian tumor could not be determined because of the small numbers of patients involved.

DISCUSSION

Eliminating high ^{18}F-FDG activity in the urinary tract is important in the diagnosis of pelvic tumors using ^{18}F-FDG PET. Several previous studies reported the usefulness of irrigation in the ^{18}F-FDG PET diagnosis of locally recurrent rectal cancer (*13,14*). However, to our knowledge, only a few studies have evaluated the usefulness of combining

TABLE 1
Details on All 41 Patients

Patient no.	Disease	Mass lesion	Tissue	SUV	Residual ^{18}F-FDG activity	
					Bladder	Ureter
1	UCer	Primary lesion	SCC	2.09	−	−
2	UCer	Primary lesion	SCC	3.41	−	+
3	UCer	Primary lesion	SCC	4.35	−	−
4	UCer	Primary lesion	SCC	4.35	−	−
5	UCer	Primary lesion	SCC	4.82	−	−
6	UCer	Primary lesion	SCC	5.96	−	−
7	UCer	Primary lesion	SCC	6.56	−	+
8	UCer	Primary lesion	SCC	7.19	−	−
9	UCer	Primary lesion	SCC	7.56	−	+
10	UCer	Primary lesion	SCC	7.97	−	−
11	UCer	Primary lesion	SCC	8.15	−	−
12	UCer	Primary lesion	SCC	10.83	−	−
13	UCer	Primary lesion	SCC	11.00	−	−
14	UCer	Primary lesion	SCC	11.53	−	−
15	UCer	Primary lesion	SCC	13.58	−	+
16	RUCer	Local recurrence	SCC	2.14	−	−
17	RUCer	Local recurrence	Clear cell adenocarcinoma	2.14	−	−
18	RUCer	Local recurrence	SCC	2.29	−	−
19	RUCer	Local recurrence	SCC	2.83	−	−
20	RUCer	Local recurrence	SCC	3.10	−	−
21	NRUCer	Pelvic cavity	Diagnosed by clinical course	0.26	−	−
22	NRUCer	Local lesion	Diagnosed by clinical course	1.69	−	−
23	NRUCer	Local lesion	No malignancy	1.95	+	−
24	UCor	Primary lesion	Adenocarcinoma	2.64	−	+
25	UCor	Primary lesion	Endometrioid adenocarcinoma	2.74	−	−
26	UCor	Primary lesion	Adenocarcinoma	4.77	−	−
27	UCor	Primary lesion	Endometrioid adenocarcinoma	4.93	−	−
28	UCor	Primary lesion	Adenocarcinoma	7.50	−	−
29	UCor	Primary lesion	Endometrioid adenocarcinoma	10.06	−	−
30	RUCor	Local recurrence	Metastatic adenocarcinoma	7.60	−	−
31	RUCor	Local recurrence	Endometrioid adenocarcinoma	11.20	−	−
32	OC	Primary lesion	Serous cystadenocarcinoma	6.36	−	−
33	ROC	Remaining ovary	Yolk sac tumor recurrence	2.60	+	−
34	ROC	Lymph node	Endometrioid adenocarcinoma	5.84	−	−
35	ROC	Lymph node	Mucinous cystadenocarcinoma	8.55	−	−
36	ROC	Lymph node	Mucinous cystadenocarcinoma	3.53	−	−
37	ROC	Lymph node	Clear cell carcinoma	5.11	−	−
38	BO	Primary lesion	Dermoid cyst	1.37	−	+
39	BO	Primary lesion	Fibroma	3.93	−	−
40	BO	Remaining ovary	No malignancy	1.17	−	−
41	BO	Remaining ovary	No malignancy	1.63	−	−

UCer = uterine cervical carcinoma; SCC = squamous cell carcinoma; RUCer = recurrent uterine cervical carcinoma; NRUCer = nonrecurrent uterine cervical carcinoma; UCor = uterine corpus carcinoma; RUCor = recurrent uterine corpus carcinoma; OC = ovarian cancer; ROC = recurrent ovarian cancer; BO = benign ovarian tumor or no malignancy.

^{18}F-FDG PET with bladder irrigation for the diagnosis of primary gynecologic tumors (*7,8,15,16*).

It was previously reported that water loading and intravenous diuretic administration could decrease retention of ^{18}F-FDG in the urinary tract (*11*) and that diuretic administration with placement of a catheter in the bladder was effective in eliminating image artifacts originating from the urinary tract (*17*). Sugawara et al. reported that the acquisition of postvoid images immediately after urination decreased the artifact due to ^{18}F-FDG accumulation in the urinary bladder, resulting in a satisfactory diagnostic ability with 100% sensitivity (*6*). Although these methods decreased the artifact due to residual ^{18}F-FDG in the urinary bladder, more than a little ^{18}F-FDG still remained in the urinary bladder. Because gynecologic tumors often exist next to the urinary bladder and sometimes invade it, differentiation of residual ^{18}F-FDG in the urinary bladder from ^{18}F-FDG accumulation in the primary tumor can be difficult. In comparison with the use of filtered backprojection for the reconstruction of ^{18}F-FDG PET images, ordered-subsets

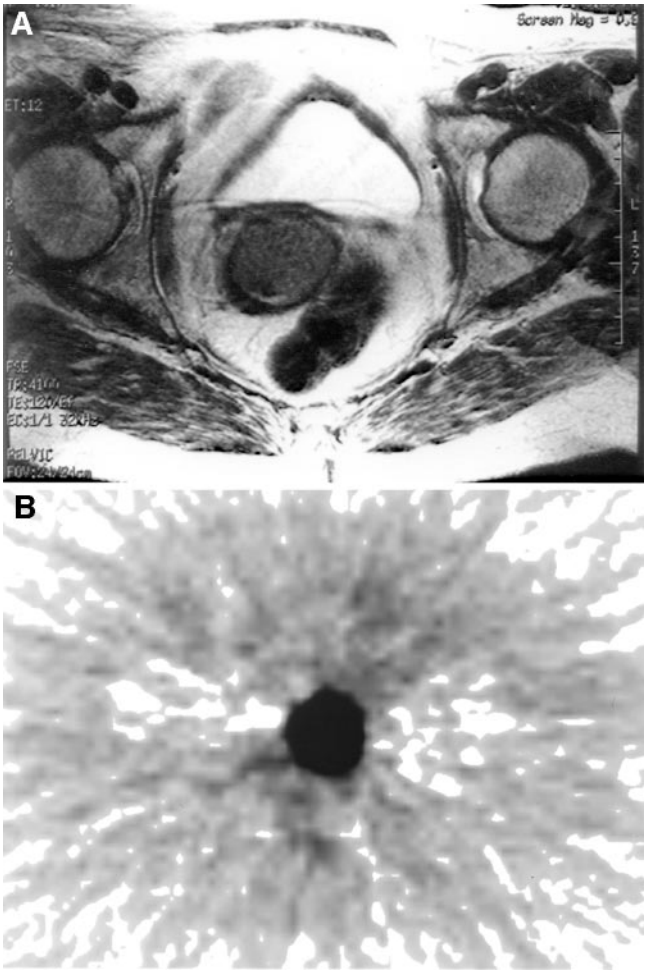

FIGURE 1. Typical case of malignant cervical cancer (patient 15). Patient was 83-y-old woman who consulted our hospital because of chief complaint of abnormal genital bleeding. (A) MRI revealed mass measuring 3 cm in diameter in cervical region of uterus. (B) ^{18}F-FDG PET images showed marked ^{18}F-FDG accumulation (SUV = 13.58) in region identical to that of mass detected by MRI. Although MRI showed urinary bladder at level similar to that of mass, ^{18}F-FDG in urinary bladder was eliminated by bladder irrigation, which facilitated evaluation of PET images. Diagnosis of squamous cell carcinoma was established on basis of biopsy results.

expectation maximization (OS-EM) has been shown to improve image quality (*18*). Reconstruction performed with OS-EM may reduce the artifact caused by high ^{18}F-FDG activity in the urinary bladder. However, even the use of this technique may not always make it easy to differentiate the residual activity from tumor ^{18}F-FDG accumulation.

As shown by our results, the ^{18}F-FDG activity in the urinary system was eliminated in most instances, making the decision on whether there was ^{18}F-FDG accumulation in tumor easy. In the 8 patients with residual activity in the urinary tract, including the 1 patient in whom the artifact was caused by high residual activity, as shown in Figure 2A, it was easy to differentiate residual activity from ^{18}F-FDG accumulation in tumor. Therefore, the residual ^{18}F-FDG

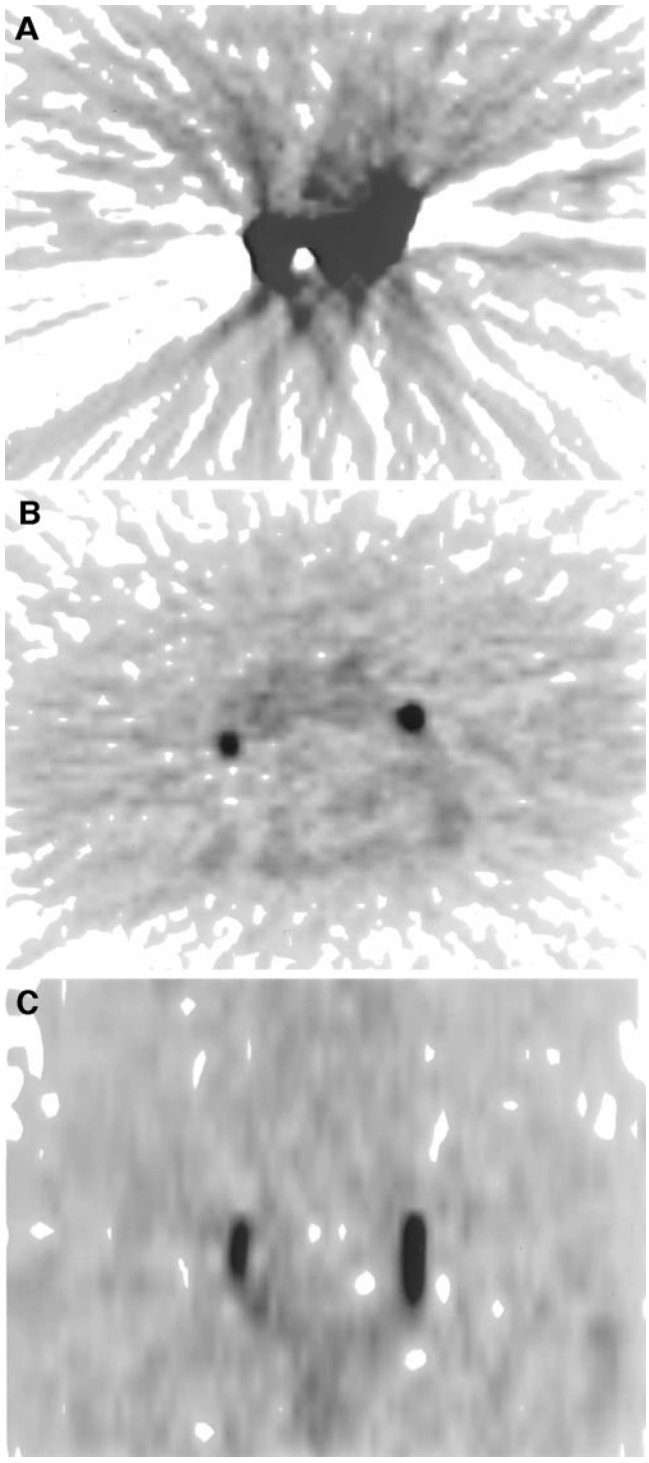

FIGURE 2. (A) Strong artifact caused by residual ^{18}F-FDG activity in urinary bladder because of insufficient bladder irrigation (patient 33). Detection of tumor ^{18}F-FDG accumulation was easy because slice level of tumor ^{18}F-FDG accumulation was not same as slice level of artifact. (B) Residual ^{18}F-FDG detected in left and right ureters after bladder irrigation (patient 24). One cannot easily differentiate ^{18}F-FDG accumulation in ureter from that in metastatic lymph node by these axial images alone. (C) Reconstruction of coronal images facilitates diagnosis of ^{18}F-FDG accumulation in ureters.

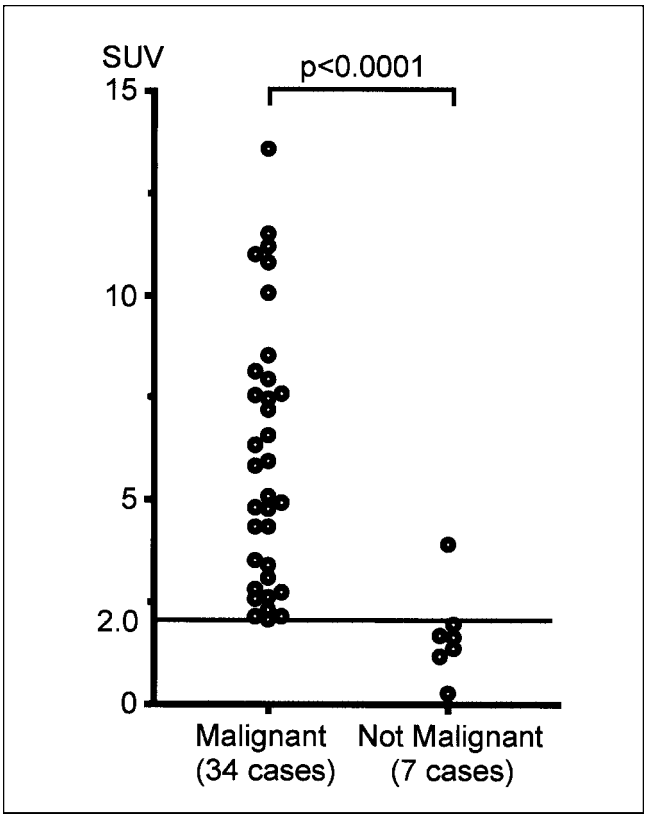

FIGURE 3. Distribution of SUVs for malignant and nonmalignant cases. Significant difference existed between SUVs for malignant cases and those for nonmalignant cases. SUV cutoff of 2.0 was optimal for differentiating malignant cases from nonmalignant cases, but there was still only 1 false-positive case of ovarian fibroma.

activity in the urinary tract had no influence on diagnosis in this study. Some disadvantages are thought to accompany the use of urinary bladder irrigation, such as increased pain during balloon catheter insertion, pain during urinary bladder irrigation, and increased radiation exposure to the technician performing the irrigation. However, no patients complained of pain during bladder irrigation in this study. Bladder irrigation is therefore thought to be a useful tool in diagnosing gynecologic tumors with ^{18}F-FDG PET.

SUVs were also used to evaluate the usefulness of ^{18}F-FDG PET in distinguishing malignant from benign gynecologic lesions. When the presence or absence of malignancy was evaluated using an SUV cutoff of 2.0, the highest diagnostic accuracy obtained was 98%. To our knowledge, most previous gynecologic studies have evaluated the accuracy of various procedures only for visual diagnosis of gynecologic tumors (*7,9,10,12*). A study of ovarian cancer reported by Hubner et al. and a study of uterine cervical cancer reported by Sugawara et al. are the only studies using quantitative analysis of SUV of which we are aware (*6,8*). Sugawara et al. reported that all uterine cervical cancer patients they examined had a mean SUV higher than 2.0 (*6*), whereas Hubner et al. reported that the accuracy of ^{18}F-FDG PET was 77% when they established an SUV cutoff of 3.0 to differentiate malignant ovarian cancer from benign tumors (*8*). Indeed, this study was limited because of the heterogeneity of the patients included, but an SUV cutoff of 2.0 had been suggested by the findings of other studies. When this cutoff value was used, only 1 patient, with an ovarian fibroma and an SUV of 3.93, was evaluated as a false-positive case. Ovarian fibroma consists of fiber cells, fibroblasts, and surrounding collagenous interstitium. Because ^{18}F-FDG was reported to accumulate in fibroblasts (*19*), increased ^{18}F-FDG accumulation was thought to be

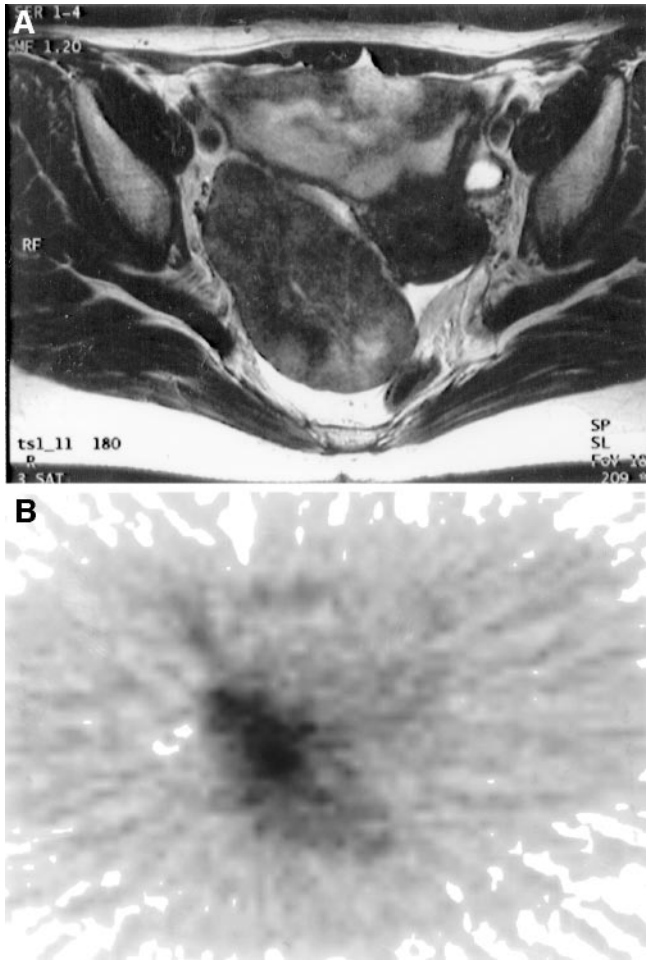

FIGURE 4. Patient was 43-y-old woman who consulted our hospital because of chief complaint of large palpable intrapelvic tumor (patient 39). MRI showed huge mass in front of sacrum and on right side of uterus. On basis of its location, mass was considered to be ovarian tumor. (A) This mass generally showed low intensity on T1- and T2-weighted images, suggesting that it contained fibrous components. However, high-intensity area was shown inside mass on T2-weighted image. MRI failed to differentiate whether mass was malignant or benign. (B) ^{18}F-FDG PET showed heterogeneous ^{18}F-FDG accumulation (SUV = 3.93) in this mass lesion, but high ^{18}F-FDG accumulation was not seen in area of strong T2 signal. On basis of these findings, malignancy could not be excluded. After surgical treatment, mass was histologically diagnosed as fibroma. This case was the only false-positive case evaluated by SUV.

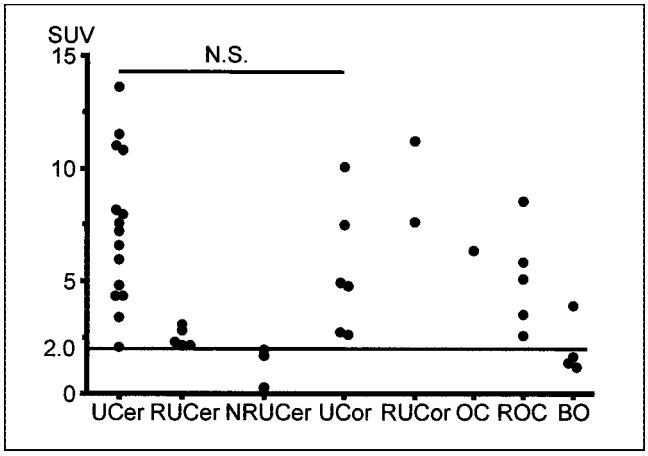

FIGURE 5. Distribution of SUVs for each gynecologic tumor. SUVs for all malignant lesions were greater than 2.0. No significant difference existed between SUVs for uterine cervical carcinomas and those for uterine corpus carcinomas. BO = benign ovarian tumor or no malignancy; NRUCer = nonrecurrent uterine cervical carcinoma; OC = ovarian cancer; ROC = recurrent ovarian cancer; RUCer = recurrent uterine cervical carcinoma; RUCor = recurrent uterine corpus carcinoma; UCer = uterine cervical carcinoma; UCor = uterine corpus carcinoma.

observed in the patient with benign ovarian fibroma. There were no significant differences in SUV between patients with uterine cervical cancer and those with uterine corpus cancer, but the SUV tended to be lower in patients with recurrent uterine cervical cancer than in those with recurrent uterine corpus cancer. That finding was probably, but not with certainty, related to their proliferation activity of tumors.

In the examination of gynecologic tumors—and especially in the diagnosis of malignant primary uterine cervical carcinoma and uterine corpus carcinoma—internal examination, smear testing, and MRI are useful. Thus, the clinical significance of the addition of ^{18}F-FDG PET may be limited. Besides us, Sugawara et al. and Umesaki et al. demonstrated the usefulness of ^{18}F-FDG PET for diagnosing recurrent uterine cervical carcinoma (*6*,*15*,*16*) and Kubik-Huch et al. reported that ^{18}F-FDG PET was useful for diagnosing recurrent ovarian cancer (*9*). For these recurrent gynecologic tumors that are considered to be difficult to diagnose by other modalities, the addition of ^{18}F-FDG PET may be useful.

CONCLUSION

When combined with continuous urinary bladder irrigation to avoid the artifact of intense ^{18}F-FDG activity in the urinary system, ^{18}F-FDG PET is a valuable diagnostic tool for detecting primary or recurrent gynecologic tumors and for differentiating malignant from nonmalignant lesions.

ACKNOWLEDGMENTS

We thank the PET chemistry staff and the PET imaging technologists at Osaka City University for their contribution to this study. We also thank the personnel of the Department of Gynecology and Obstetrics for their cooperation.

REFERENCES

1. Bida GT, Satyamurthy N, Barrio JR. The synthesis of 2-[F-18]fluoro-2-deoxy-D-glucose using glycols: a reexamination. *J Nucl Med.* 1984;25:1327–1334.
2. Di Chiro G. Positron emission tomography using [^{18}F] fluorodeoxyglucose in brain tumors: a powerful diagnostic and prognostic tool. *Invest Radiol.* 1987;22:360–371.
3. Burk D, Woods M, Hunter J. On the significance of glucolysis for cancer growth, with special reference to Morris rat hepatomas. *J Natl Cancer Inst.* 1967;38:839–863.
4. Knox WE, Jamdar SC, Davis PA. Hexokinase, differentiation and growth rates of transplanted rat tumors. *Cancer Res.* 1970;30:2240–2244.
5. Strauss LG, Conti PS. The applications of PET in clinical oncology. *J Nucl Med.* 1991;32:623–650.
6. Sugawara Y, Eisbruch A, Kosuda S, Recker BE, Kison PV, Wahl RL. Evaluation of FDG PET in patients with cervical cancer. *J Nucl Med.* 1999;40:1125–1131.
7. Casey MJ, Gupta NC, Muths CK. Experience with positron emission tomography (PET) scans in patients with ovarian cancer. *Gynecol Oncol.* 1994;53:331–338.
8. Hubner KF, McDonald TW, Niethammer JG, Smith GT, Gould HR, Buonocore E. Assessment of primary and metastatic ovarian cancer by positron emission tomography (PET) using 2-[^{18}F]deoxyglucose (2-[^{18}F]FDG). *Gynecol Oncol.* 1993;51:197–204.
9. Kubik-Huch RA, Dorffler W, von Schulthess GK, et al. Value of (^{18}F)-FDG positron emission tomography, computed tomography, and magnetic resonance imaging in diagnosing primary and recurrent ovarian carcinoma. *Eur Radiol.* 2000;10:761–767.
10. Karlan BY, Hawkins R, Hoh C, et al. Whole-body positron emission tomography with 2-[^{18}F]-fluoro-2-deoxy-D-glucose can detect recurrent ovarian carcinoma. *Gynecol Oncol.* 1993;51:175–181.
11. Grab D, Flock F, Stohr I, et al. Classification of asymptomatic adnexal masses by ultrasound, magnetic resonance imaging, and positron emission tomography. *Gynecol Oncol.* 2000;77:454–459.
12. Yuan CC, Liu RS, Wang PH, Ng HT, Yeh SH. Whole-body PET with (fluorine18)-2-deoxyglucose for detecting recurrent ovarian carcinoma: initial report. *J Reprod Med.* 1999;44:775–778.
13. Flamen P, Stroobants S, Van Cutsem E, et al. Additional value of whole-body positron emission tomography with fluorine-18-2-fluoro-2-deoxy-D-glucose in recurrent colorectal cancer. *J Clin Oncol.* 1999;17:894–901.
14. Miraldi F, Vesselle H, Faulhaber PF, Adler LP, Leisure GP. Elimination of artifactual accumulation of FDG in PET imaging of colorectal cancer. *Clin Nucl Med.* 1998;23:3–7.
15. Umesaki N, Tanaka T, Miyama M, et al. The role of ^{18}F-fluoro-2-deoxy-D-glucose positron emission tomography (^{18}F-FDG-PET) in the diagnosis of recurrence and lymph node metastasis of cervical cancer. *Oncol Rep.* 2000;7:1261–1264.
16. Umesaki N, Tanaka T, Miyama M, et al. Early diagnosis and evaluation of therapy in postoperative recurrent cervical cancers by positron emission tomography. *Oncol Rep.* 2000;7:53–56.
17. Leisure GP, Vesselle HJ, Faulhaber PF, O'Donnell JK, Adler LP, Miraldi F. Technical improvements in fluorine-18-FDG PET imaging of the abdomen and pelvis. *J Nucl Med Technol.* 1997;25:115–119.
18. Meikle SR, Bailey DL, Hooper PK, et al. Simultaneous emission and transmission measurements for attenuation correction in whole-body PET. *J Nucl Med.* 1995;36:1680–1688.
19. Kubota K, Kubota R, Yamada S. FDG accumulation in tumor tissue. *J Nucl Med.* 1993;34:419–421.

JNM The Journal of NUCLEAR MEDICINE

Evaluation of ^{18}F-FDG PET with Bladder Irrigation in Patients with Uterine and Ovarian Tumors

Koichi Koyama, Terue Okamura, Joji Kawabe, Nozomi Ozawa, Kenzi Torii, Naohiko Umesaki, Masato Miyama, Hironobu Ochi and Ryusaku Yamada

J Nucl Med. 2003;44:353-358.

The Journal of Nuclear Medicine is published monthly.
SNMMI | Society of Nuclear Medicine and Molecular Imaging
1850 Samuel Morse Drive, Reston, VA 20190.
(Print ISSN: 0161-5505, Online ISSN: 2159-662X)

SNMMI SOCIETY OF NUCLEAR MEDICINE AND MOLECULAR IMAGING